Red blood cell dynamics during malaria infection violate the assumptions of mathematical models of infection dynamics

Madeline A.E. Peters [1,2], **Aaron A. King** [2,3,4,5] **and Nina Wale** [1,6,7,*]

[1] *Department of Microbiology, Genetics & Immunology, Michigan State University, East Lansing, Michigan, USA*
[2] *Department of Ecology & Evolutionary Biology, University of Michigan, Ann Arbor, Michigan, USA*
[3] *Center for the Study of Complex Systems, University of Michigan, Ann Arbor, Michigan, USA*
[4] *Department of Mathematics, University of Michigan, Ann Arbor, Michigan, USA*
[5] *Santa Fe Institute, Santa Fe, New Mexico, USA* [6] *Department of Integrative Biology, Michigan State University, East Lansing, Michigan, USA* [7] *Program in Ecology, Evolution and Behavior, Michigan State University, East Lansing, Michigan, USA*

Correspondence*:
Nina Wale
walenina@msu.edu

ABSTRACT

For decades, mathematical models have been used to understand the course and outcome of malaria infections (i.e., infection dynamics) and the evolutionary dynamics of the parasites that cause them. A key conclusion of these models is that red blood cell (RBC) availability is a fundamental driver of infection dynamics and parasite trait evolution. The extent to which this conclusion holds will in part depend on model assumptions about the host-mediated processes that regulate RBC availability i.e., removal of uninfected RBCs and supply of RBCs. Diverse mathematical functions have been used to describe host-mediated RBC supply and clearance, but it remains unclear whether they adequately capture the dynamics of RBC supply and clearance during infection. Here, we use a unique dataset, comprising time-series measurements of erythrocyte (i.e., mature RBC) and reticulocyte (i.e., newly supplied RBC) densities during *Plasmodium chabaudi* malaria infection, and a quantitative data-transformation scheme to elucidate whether RBC dynamics conform to common model assumptions. We found that RBC clearance and supply are not well described by mathematical functions commonly used to model these processes. Furthermore, the temporal dynamics of both processes vary with parasite growth rate in a manner again not captured by existing models. Together, these finding suggest that new model formulations are required if we are to explain and ultimately predict the within-host population dynamics and evolution of malaria parasites.

Keywords: ***Plasmodium chabaudi*, malaria, growth rate, erythropoiesis, red blood cells, host response**

1 INTRODUCTION

Red blood cells (RBCs) are the primary target cells of malaria parasites during the blood-stage of infection and their availability changes dramatically over an infection's course (Lamb and Langhorne, 2008; Timms et al., 2001; Mackinnon and Read, 1999; Wale et al., 2017). These changes are caused by parasite destruction of RBCs, as well as a suite of host responses (reviewed in Deroost et al., 2016), and can have profound consequences for both host health and parasite fitness e.g., underlying the characteristic anemia of malaria infections. As such, quantitatively understanding the causes and consequences of RBC dynamics *in vivo* is essential if we are to explain the disease and dynamics of malaria infections.

Over the last three decades, mathematical models have been used to quantitatively understand the various mechanisms by which variation in RBC dynamics comes about and the consequences of this variation for the population dynamics and evolution of malaria parasites (reviewed in Khoury et al. (2018)). For example, Jakeman et al. (1999) used a mathematical model to suggest that the anemia of malaria infections results primarily from destruction of uninfected RBCs, rather than from direct destruction by parasites or impaired RBC production (dyserythropoiesis). Others have elucidated the consequences of anemia for the population dynamics and evolution of malaria parasites. Theoretical studies have posited that anemia induces RBC limitation, resulting in the cessation of parasite growth and intense inter-parasite competition for RBCs (McQueen and McKenzie, 2004; Mideo et al., 2008). Over evolutionary time, these competitive interactions are hypothesized to have driven selection for parasite traits that impact host health, such as the preference of different species for different ages of RBCs ("age preference") and growth rate (De Roode et al., 2005; Antia et al., 2008; Pak et al., 2023).

Critically, the robustness of model-derived inferences about the disease and dynamics of malaria infections depend on the validity of assumptions underlying those models (Childs and Buckee, 2015; Peters et al., 2021). In particular, assumptions about the processes by which RBCs are supplied and cleared will be especially important, since these processes are major drivers of the availability and age-structure of RBCs. The vast majority of studies describe RBC supply and uninfected RBC (uRBC) clearance as a constant and/or as a function of RBC abundance (Table 1, Figure 1A). For example, the supply of immature RBCs (reticulocytes) is most often modeled as a constant function of time (Anderson et al., 1989; Gravenor et al., 1995; Lim et al., 2013; Khoury et al., 2018) or as an increasing linear function of the deficit in RBC (erythrocyte) density (a "homeostatic" model) (Greischar et al., 2016; Khoury et al., 2018; Haydon et al., 2003; Mideo et al., 2008). Although these assumptions are appealing in their simplicity and have been necessitated by the technical challenges of quantifying the dynamics of RBC supply and clearance *in vivo*, recent work implies that these simple, linear functions may not best represent RBC dynamics. For example, recent empirical work suggests that the immunohematological processes responsible for RBC supply change dramatically upon infection and may vary with parasite traits (Ruan and Paulson, 2023; Lamb and Langhorne, 2008; Lin et al., 2017; Wale et al., 2017).

Here, we investigate the validity of commonly invoked assumptions about RBC supply and clearance, using a unique dataset and data-transformation scheme that permit us to quantify these regulatory processes throughout the course of infection. We find that mathematical functions commonly used to describe RBC supply and clearance do not capture the data well. Our results suggest we need new empirical methods and modeling strategies if we are to fully understand malaria infection dynamics and evolution.

2 MATERIALS AND METHODS

Here, we conduct a new analysis of a previously published dataset and model to elucidate (i) to what extent the functions commonly used to describe RBC supply and clearance conform to standard assumptions and (ii) whether these functions change with parasite growth rate. Full details about the model and the data can be found in Wale et al. (2019). We describe each briefly below.

2.1 Hosts and parasites

Hosts were 6- to 8-week old C57BL/6J female mice. 12 mice were infected with 10^6 *Plasmodium chabaudi* parasites of a pyrimethamine-resistant strain denoted AS_{124}. To generate variation in the growth rate and dynamics of infection, groups of 3 mice each received either a 0.05% (high), 0.005% (medium), 0.0005% (low) or 0% (unsupplemented) solution of *para*-aminobenzoic acid (pABA) as drinking water, initiated a week prior to parasite inoculation. pABA is not a nutrient for the host but significantly increases parasite growth rate (Fenton et al., 1950; Wale et al., 2017), as we saw during this experiment (Wale et al., 2019); we thus refer to it as a "parasite nutrient", hereafter. Infections were monitored daily from day 0 (i.e., the day of inoculation) to day 20 post-inoculation (PI). Following daily blood sampling from the tail, parasite densities, erythrocyte densities and reticulocyte densities were quantified via quantitative PCR, Coulter counting and flow cytometry (Figure 2A). One mouse in the high pABA treatment died on day 8. One mouse in each of the high and medium treatments received fewer parasites than was intended; they were omitted from our analyses. The experiment was reviewed by the Institutional Animal Care and Use Committee of Pennsylvania State University, where the experiment was conducted (IACUC protocol 44512-1, P.I. Dr. A Read).

2.2 Data transformation

To quantify the host RBC supply and clearance responses during infection, we used the approach first presented in Wale et al. (2019). Notably, rather than generating quantitative *predictions* of malaria infection dynamics (*a la* the refs. in Table 1), this approach transforms three data streams (erythrocytes, reticulocytes, parasites; Figure 2A) into three host-responses, which together determine the supply and clearance of RBCs (Figures 2Bii,iv,v). We thus refer to this approach as a "data transformation scheme", as opposed to a model.

The equations posit that

$$E_{t+1} = (R_t + E_t)\,\exp\left(-\frac{M_t + N_t}{R_t + E_t}\right),$$
$$M_{t+1} = \beta\, K_t\,\exp\left(-\frac{W_t + N_t}{R_t + E_t}\right),$$
$$K_t = (R_t + E_t)\left(1 - \exp\left(-\frac{M_t}{R_t + E_t}\right)\right),$$

where, on day t post-infection, E_t and R_t are unparasitized erythrocyte and reticulocyte densities, respectively, M_t is merozoite density and K_t is the density of parasitized RBCs. These equations express the assumptions that (i) reticulocytes entering circulation on day t mature to become erythrocytes on day $t+1$ (Ney, 2011), (ii) *P. chabaudi* merozoites attack unparasitized RBCs without respect to age (Jarra and Brown, 1989; Yap and Stevenson, 1994), (iii) parasitized RBCs burst in one day to produce β merozoites on average, (iv) parasitized RBCs are removed by the immune system at a rate dependent on the time-varying

quantity W_t, and (v) irrespective of their parasitization status, RBCs are removed from circulation at a rate dependent on the time-varying quantity N_t.

The transformation is regularized by assuming that the time-dependent functions $\log R_t$, $\log W_t$ and $\log N_t$ are Gaussian Markov random fields (GMRF), each with its own intensity, and that the measured values of reticulocyte, RBC and parasitized cell densities on day t are log-normally distributed about R_t, $R_t + E_t$, and K_t, respectively. The GMRF intensities, error standard deviations and initial conditions were estimated from the data using iterated filtering using the **R** package **pomp** (King et al., 2016; Ionides et al., 2015). 2000 samples from the smoothing distribution for each of these variables were drawn for each individual infected mouse (Figure 2B). Full details of these computations are provided in the original paper and its supplement (Wale et al., 2019); the code for the computations in this paper are archived on GitHub at `https://github.com/kingaa/bdd/tree/master/nw11_hier/bioRxiv2024`.

2.3 Estimating clearance rate

In the majority of modeling studies, clearance rate is defined as the rate at which uninfected RBCs (uRBCs) are cleared. Accordingly, we use the output of our data-transformation scheme to estimate Q_t^{un}, the probability on a given day t that an individual uRBC will be cleared by indiscriminate killing. We first define S_t^M, the probability that an RBC escaped infection by a malaria parasite and S_t^N, the probability that an RBC is not cleared by indiscriminate killing as:

$$S_t^M = \exp\left(-\frac{M_t}{R_t + E_t}\right), \qquad S_t^N = \exp\left(-\frac{N_t}{R_t + E_t}\right).$$

The probability that an uninfected RBC is cleared by indiscriminate killing on day t is then

$$Q_t^{\text{un}} = S_t^M \left(1 - S_t^N\right).$$

2.4 Estimating treatment-level RBC supply and clearance

To examine whether RBC supply and clearance dynamics change with parasite nutrient treatment (and hence parasite growth rate), while accounting for intra- and inter-mouse variation, we performed the following analysis (Figures 2C-D). The data-transformation scheme yielded a distribution of 2000 supply and clearance trajectories for each mouse (Figure 2B), each with an associated likelihood (e.g., Figure 2C, 300 trajectories displayed for ease of interpretation). We calculated the relative likelihood of each trajectory by comparing each likelihood to the maximum likelihood for a given mouse. Finally, grouping the trajectories by treatment, we used the `wquant` function from the **pomp** package (King et al., 2016) to calculate weighted quantiles (5%, 50% and 95%), using the relative likelihoods as sampling weights. We thus captured the treatment-specific dynamics of the RBC supply and clearance responses, while accounting for uncertainty in the fitting of the data-transformation scheme.

2.5 Regression analysis of the RBC supply function

Visualization of the relationship between R_t and E_{t-1} suggested that the relationship between R_t and E_{t-1} might be best described by two functions rather than one (cf. *Results*; Figure 3), i.e., that RBC supply are supplied in two distinct phases and, furthermore, that it may change with parasite nutrient treatment. To investigate these possibilities, we built a suite of 30 regression models differing in their inclusion of terms dictating (a) whether or not the RBC supply response was uni- or bi-phasic (phase); (b)

the day post-infection on which the two phases begin/end (breakpoint; either 8, 9, 10, 11, or none, in the case of the uniphasic model); (c) the shape of the relationship between R_t and E_{t-1} (linear, nonlinear), and (d) whether its shape changes with parasite nutrient treatment (pABA).

We fit these statistical models to the supply/clearance rate trajectories, as estimated from the data-transformation scheme. To account for variation in the shape of the 2000 trajectories outputted in the scheme-fitting process (Figure 2, Figure S2, *Supplementary Material*), we used a bootstrapping approach. Specifically, we fit each regression model to 1000 "datasets", each of which contained a single trajectory from each of the ten mice. To construct each dataset, we sampled one trajectory per mouse such that the probability that a trajectory was sampled was proportionate to its relative likelihood. The models were then fit to each dataset in turn and the best fit model selected via AIC. Note that to address the issue of multicollinearity associated with regressing against higher order polynomials, we opted to use orthogonal polynomials for model fitting.

2.6 The dynamics of RBC clearance rate and reticulocyte supply during infection

To investigate whether (i) clearance rate of uninfected RBCs (Q_t^{un}) and (ii) reticulocyte supply changes through time and/or with parasite nutrient (pABA) treatment, we again performed a bootstrap analysis. For the analysis of clearance rate dynamics, we compared five generalized additive models (`gam`) that described Q^{un} as: (A) a constant function (Table 3); (B) a smooth function of time, i.e., day post-infection; (C) a smooth function of time and pABA treatment; (D) a linear function of erythrocyte density; or (E) a linear function of erythrocyte density and pABA treatment. For the analysis of reticulocyte dynamics, we fitted only Models A-C (Table 3). Again, the models were fit to 1000 datasets, each composed of ten trajectories and sampled as described above. Model fitting was performed using the **mgcv** package in **R** (Wood, 2017; R Core Team, 2022); model selection was performed using AIC.

3 RESULTS

Host supply and destruction of uninfected RBCs are major drivers of the availability of RBCs during infection. We set out to examine (i) whether mathematical functions that are used to describe these processes (Table 1, Figure 1) capture the data and (ii) whether they change with an experimental treatment (dietary pABA supply) that impacts parasite growth rate but has no effect on the host (Figure S1, *Supplementary Material*). To do so, we analyzed time-series data used a data-transformation scheme that allows us to quantify host RBC supply and clearance responses through time. Specifically, this analysis generated a distribution of response trajectories for each mouse, each of which was associated with a likelihood (Figure 2B). By analyzing this distribution we can quantify the shape of the functions that describe RBC supply and clearance while accounting for the fact that multiple realizations of the data-transformation scheme may explain the data.

3.1 RBC supply is better described by a biphasic function of erythrocyte density than a single function

RBC supply is commonly modeled as single, decreasing function of (lagged) erythrocyte density or as a constant (Figure 1A). These models hypothesize that— if we plot reticulocyte (i.e., newly supplied RBC) density against lagged erythrocyte density— we will yield a single curve (Figure 1A). Contrary to this hypothesis, however, we found that the R_t-E_{t-1} curve takes the form of a loop (Figure 3). The "loop" shape of the R-E curves suggests that RBC supply is not well described by a single function.

We surmised from the shape of this loop that RBC supply may instead occur in two distinct phases that start/end about ∼half-way through the first 20 days post-infection. To investigate this hypothesis, we conducted a regression analysis. Specifically, we compared a suite of models that allowed us to ask (i) whether or not RBC supply occurs in two phases, (ii) if it occurs in two phases, at what time (i.e., day post-infection) represents the "breakpoint" between the two phases, (iii) whether the R_t supply is a linear or curved function of E_{t-1} and (iv) whether it changes with supplementation of a nutrient that changes parasite growth rate (Table 2).

We found overwhelming support for the hypothesis that RBC supply occurs in two phases, rather than one: in 1000 iterations of our regression analysis, the single phase model was never selected. Instead, our analysis strongly suggests that the RBC supply regimen changes at day 9 (98.9% of models selected specify a breakpoint at day 9; Figure 4A), whereupon there is a marked shift in the rate at which RBCs are supplied. For example— according to our top model— while ~ 55 reticulocytes are supplied per day for every 1000 erythrocytes lost in the first phase (Figure 4B, "Phase 1"), in the second ~ 420 reticulocytes are supplied for every 1000 erythrocytes lost (Figure 4B, "Phase 2").

We found weak support for the hypothesis that RBC supply regimen changes with pABA treatment (Figures 4D-E, Models E and B, favored in 13.5% and 8.9% of iterations respectively). According to these models, mice supplemented with high concentrations of the parasite nutrient produce more reticulocytes at a given erythrocyte density than those supplemented with low concentrations (yellow and green versus blue and orange series, Figures 4D-E).

To further investigate the impact of pABA on RBC supply dynamics during infection, we compared a suite of generalized additive models (Table S1, *Supplementary Material*). This analysis strongly suggests that reticulocyte supply varies with both time and pABA treatment (Model A, winning best support in 95.9% of model selection iterations). Specifically, reticulocyte concentrations are higher prior to day 7, and reach a higher peak, in mice supplemented with pABA (i.e., with fast growing parasites; Figures S2A,C)

3.2 RBC clearance rate is not well described by commonly employed functions

Similarly, we found that commonly employed functions (Figure 1B) poorly describe the dynamics of RBC clearance during infection. Visualization of the RBC clearance trajectories suggest that RBC clearance varies markedly with time, beginning at a relatively constant rate, before increasing sharply and peaking around day 11-12, and may vary with parasite nutrient treatment (Figure 5A). To investigate this hypothesis, we again performed a bootstrapped regression analysis. This revealed similar support for two hypotheses: (1) that uninfected RBC clearance rate Q^{un} changes with time and parasite nutrient treatment (Model A, Table 3, 52.3% of models selected) and (2) that clearance rate changes with time (Model B, Table 3, 47.7% of models selected). According to the best-supported model, the zenith in clearance rate is higher in mice supplemented with high concentrations of parasite nutrients (Figure 5A). Importantly, a model of constant clearance rate was never selected, and neither was a model that describes clearance rate as a linear function of erythrocyte density. (Figure 5B).

4 DISCUSSION

Mathematical models have shaped our understanding of diverse phenomena in malaria biology— from the dynamics of infections (Haydon et al., 2003; Wale et al., 2019; Kochin et al., 2010; Mideo et al., 2008), to the evolution of transmission investment (i.e., gametocyte production) (Greischar et al., 2016) and the design of control interventions (Camponovo et al., 2021). In this work, we find that common model

assumptions about the processes that regulate RBC abundance during infection do not hold. First, we find that RBC supply is not well described as a single function of RBC deficit as is commonly assumed (Table 1); rather it is better described as a two functions (at a minimum) that roughly describe the first and second half of the acute phase of infection. Second, and similarly, we find that RBC clearance is poorly described by commonly proscribed linear functions and may be better captured with time-varying and/or biphasic functions. Finally, our analysis suggests that RBC supply and clearance may change with parasite growth rate (as manipulated via host nutrition).

This mismatch between model assumptions and biology could have serious consequences for the inferences we have made about malaria infection dynamics and parasite trait evolution using mathematical models. For example, there is a longstanding debate about whether parasite population growth in the blood is primarily controlled by the availability of RBCs ("bottom-up" forces) or by immune-mediated killing (i.e., "top-down" forces) (Antia et al., 2008; Kochin et al., 2010; Wale et al., 2019; Haydon et al., 2003). Our analysis implies that RBCs may be more limiting than is often assumed, since most models have not accounted for almost complete cessation of erythropoiesis at the infection's outset (i.e., in "phase 1"). This underestimation of the importance of RBC limitation could also impact our understanding of pathogen evolution. Evolutionary theory states that— all else being equal— competition for resources (here, RBCs) impacts selection for virulence-related traits, such as growth rate or burst size (Frank, 1996; Mosquera and Adler, 1998; Bremermann and Pickering, 1983; van Baalen and Sabelis, 1995; Nowak and May, 1994). Since resource competition will be intense when RBCs are limited, we may have underestimated the strength and timing under which parasites experience selection for these traits. That said, our results make it difficult to make this speculation comfortably, for they imply that all else may not equal when it comes to resource dynamics during malaria infection. Specifically, RBC supply and clearance of RBCs may systematically vary with parasite traits (growth rate, as mediated by parasite nutrient treatment) in a manner not captured by present evolutionary theory as far as we are aware. It is difficult to intuit how such feedbacks may impact within-host competition or virulence evolution. Given this difficulty and the limited sample size of our experiment, a more robust investigation of the relationship between parasite traits and RBC dynamics is warranted.

We recognize that our inferences, although primarily data-driven, may in part reflect the assumptions of the data-transformation scheme used to generate them. However, they are unlikely to impact our central conclusion that RBC dynamics do not behave as commonly modeled. We make two key simplifying assumptions. The first is that all RBCs are equally invadable by *Plasmodium chabaudi* (Jarra and Brown, 1989; Yap and Stevenson, 1994). If parasites in fact exhibit a preference for a narrow subset of RBCs, we will have underestimated parasite-mediated destruction of RBCs (i.e., via M or W) and, as a result, overestimated the clearance of uninfected cells, Q^{un} (see *Supplementary Material* for a full explanation). The dynamics of Q^{un} are unlikely to be greatly impacted by this assumption, however. The second assumption that could affect our inference is that reticulocytes mature into erythrocytes after only one day (Ney, 2011). If reticulocytes remain immature RBCs for longer (as some studies imply (Thakre et al., 2018; Wiczling and Krzyzanski, 2008; Ganzoni et al., 1969; Gronowicz et al., 1984)), we will have "double-counted" reticulocytes and hence overestimated RBC supply at each time-point. Nonetheless, we stress that our goal here was not to present a "better", or even a predictive, model of RBC dynamics, but rather ask whether or not RBC supply and clearance conform to commonly-invoked assumptions. In light of this goal, a shift in the precise shape of the RBC supply and clearance functions are unlikely to impact our central conclusion.

Furthermore, our conclusions mirror those of recent experimental studies that suggest that RBC dynamics in the context of infection are not regulated by the same mechanisms that govern homeostasis in the absence of infectious challenge. Such immunohematological studies provide us with testable, mechanistic explanations for our observations. It is now widely recognized that the inflammatory response, as stimulated by infection, causes "stress erythropoiesis". This response is characterized by the cytokine-mediated suppression of erythropoiesis immediately following infection, an acceleration of erythrophagocytosis and finally the production of a "pulse" of RBCs in the spleen, via a heme-mediated signaling cascade (Yap and Stevenson, 1992; Chang and Stevenson, 2004; Paulson et al., 2020; Ruan and Paulson, 2023). Given that malaria infection induces (i) significant inflammation, erythrophagocytosis and heme-accumulation in the spleen, and (ii) the concordance between the timescale of stress erythropoiesis and our RBC supply curve, it is reasonable to hypothesize that similar mechanisms underlie the biphasic RBC supply dynamics we have observed. Stress erythropoiesis may also be implicated in our observation that RBC clearance increases with time, since it is associated with both accelerated production and turnover of RBCs (Libregts et al., 2011; Klei et al., 2019); furhter, anti-RBC antibodies may also be involved. (Fernandez-Arias et al., 2016; Mourão et al., 2018) Finally— and not mutually exclusively— it is also possible that the process of RBC aging changes during infection and that this provokes an acceleration of senescence-mediated RBC clearance. In birds, erythrocytes produced during infection enter the bloodstream "biologically older" than normal RBCs, i.e., they have shorter telomeres, and it is possible such a phenomenon occurs in (non-nucleated) vertebrate RBCs (Asghar et al., 2015). Alternatively, the oxidatively stressed environment of the malaria-infected bloodstream may induce physiological aging of stress erythrocytes stimulating their rapid removal (Bissinger et al., 2018).

Thus, both our analyses and empirical studies suggest that to obtain a comprehensive understanding of malaria infection dynamics and evolution requires that we refine the way we build and test mathematical models of them. We propose two avenues for future research. First, richer time-series datasets will help to inform the formulation of more biologically realistic models, as our analyses demonstrate. Historically, it has not been possible to disentangle whether a host is accelerating the clearance of RBCs (or "bystanding killing") or simply not supplying the bloodstream with RBCs: both processes result in a deficit of RBCs (as discussed in, e.g., Metcalf et al., 2011, 2012). Simply by measuring reticulocyte dynamics, we were able to disentangle these processes. We thus advocate for experimental measurements of difficult-to-infer processes that could impact our inference. For example, the maturation- and/or clearance-rate of reticulocytes could be measured via transfusion of fluorescently-labeled cells or by "double-labeling" endogenous RBCs (as in Gifford et al., 2006; Klei et al., 2019; Bennett et al., 2019). Experiments in bird hosts, whose RBCs come "prelabelled" with telomeres, could also be informative. Second, new model structures could prove valuable. For example, RBC dynamics may be described as time-varying functions as in e.g., Thakre et al. (2018), Wale et al. (2019) and Kamiya et al. (2021). It is unlikely that infection dynamics are determined by time *per se* but rather vary with a suite of underlying biological mechanisms that happen to vary with time, and the "looped" trajectory of the $R - E$ curve (and $Q^{\mathrm{un}} - E$ curve, not shown) implies that a time-dependent model will not be predictive. Ultimately, therefore it may be instructive to draw on our increasing understanding of immunohematological feedbacks and attempt to explicitly model, for example, the impact of the immune response on erythropoiesis, to better describe and predict malaria infection dynamics. Achieving this goal will be non-trivial, given the challenge of formulating simple models of immunodynamics, but will likely yield more robust inferences about the course, outcome and evolution of malaria parasites.

CONFLICT OF INTEREST STATEMENT

The authors declare that the research was conducted in the absence of any commercial or financial relationships that could be construed as a potential conflict of interest.

AUTHOR CONTRIBUTIONS

All authors contributed to the conceptualization of the manuscript, design of the methodology and design of the visualization. MAEP wrote the manuscript with AAK and NW contributing substantial revision. MAEP and AAK performed the analyses, and MAEP performed the visualization of the methods and results.

FUNDING

This work was supported by grants from the U.S. National Institutes of Health, (Grant #1R01AI143852 to AAK) and a grant from the Interface program, jointly operated by the U.S. National Science Foundation and the National Institutes of Health (Grant #1761603). This work was also supported by institutional funds to NW.

ACKNOWLEDGMENTS

We are thankful to Andrew Read and his laboratory at Penn State University, for performing the experiment that generated data for this work and Wale et al. (2019).

SUPPLEMENTAL DATA

Supplementary information, figures and tables are available in the *Supplementary Material* document.

DATA AVAILABILITY STATEMENT

The datasets as well as all code for analyses and figures for this study can be found in the "bioRxiv2024" repository on GitHub at `https://github.com/kingaa/bdd/tree/master/nw11_hier/bioRxiv2024`.

REFERENCES

Anderson, R. M., May, R. M., and Gupta, S. (1989). Non-linear phenomena in host-parasite interactions. *Parasitology* 99, S59–S79. doi:10.1017/s0031182000083426

Antia, R., Yates, A., and de Roode, J. C. (2008). The dynamics of acute malaria infections. I. Effect of the parasite's red blood cell preference. *Proc. R. Soc. Lond. B* 275, 1449–1458. doi:10.1098/rspb.2008.0198

Asghar, M., Hasselquist, D., Hansson, B., Zehtindjiev, P., Westerdahl, H., and Bensch, S. (2015). Hidden costs of infection: chronic malaria accelerates telomere degradation and senescence in wild birds. *Science* 347, 436–438. doi:10.1126/science.1261121

Bennett, L. F., Liao, C., Quickel, M. D., Yeoh, B. S., Vijay-Kumar, M., Hankey-Giblin, P., et al. (2019). Inflammation induces stress erythropoiesis through heme-dependent activation of SPI-C. *Sci. Signal.* 12, eaap7336. doi:10.1126/scisignal.aap7336

Bissinger, R., Bhuyan, A. A. M., Qadri, S. M., and Lang, F. (2018). Oxidative stress, eryptosis and anemia: a pivotal mechanistic nexus in systemic diseases. *FEBS J.* 286, 826–854. doi:10.1111/febs.14606

Bremermann, H. J. and Pickering, J. (1983). A game-theoretical model of parasite virulence. *J. Theor. Biol.* 100, 411–426. doi:10.1016/0022-5193(83)90438-1

Camponovo, F., Lee, T. E., Russell, J. R., Burgert, L., Gerardin, J., and Penny, M. A. (2021). Mechanistic within-host models of the asexual *Plasmodium falciparum* infection: a review and analytical assessment. *Malar. J.* 20, 1–22. doi:10.1186/s12936-021-03813-z

Chang, K. H. and Stevenson, M. M. (2004). Effect of anemia and renal cytokine production on erythropoietin production during blood-stage malaria. *Kidney Int.* 65, 1640–1646. doi:10.1111/j.1523-1755.2004.00573.x

Childs, L. M. and Buckee, C. O. (2015). Dissecting the determinants of malaria chronicity: why within-host models struggle to reproduce infection dynamics. *J. R. Soc. Interface* 12, 20141379. doi:10.1098/rsif.2014.1379

De Roode, J. C., Pansini, R., Cheesman, S. J., Helinski, M. E. H., Huijben, S., Wargo, A. R., et al. (2005). Virulence and competitive ability in genetically diverse malaria infections. *Proc. Natl. Acad. Sci.* 102, 7624–7628. doi:10.1073/pnas.0500078102

Deroost, K., Pham, T.-T., Opdenakker, G., and Steen, P. E. V. d. (2016). The immunological balance between host and parasite in malaria. *FEMS Microbiol. Rev.* 40, 208–257. doi:10.1093/femsre/fuv046

Fenton, P. F., Cowgill, G. R., Stone, M. A., and Justice, D. H. (1950). The nutrition of the mouse: VIII. studies on pantothenic acid, biotin, inositol and p-aminobenzoic acid. *J. Nutr.* 42, 257–269. doi:10.1093/jn/42.2.257

Fernandez-Arias, C., Rivera-Correa, J., Gallego-Delgado, J., Rudlaff, R., Fernandez, C., Roussel, C., et al. (2016). Anti-self phosphatidylserine antibodies recognize uninfected erythrocytes promoting malarial anemia. *Cell Host Microbe* 19, 194–203. doi:10.1016/j.chom.2016.01.009

Frank, S. A. (1996). Models of parasite virulence. *Q. Rev. Biol.* 71, 37–78. doi:10.1086/419267

Ganzoni, A., Hillman, R. S., and Finch, C. A. (1969). Maturation of the macroreticulocyte. *Br. J. Haematol.* 16, 119–136. doi:10.1111/j.1365-2141.1969.tb00384.x

Gifford, S. C., Yoshida, T., Shevkoplyas, S. S., and Bitensky, M. W. (2006). A high-resolution, double-labeling method for the study of in vivo red blood cell aging. *Transfusion (Paris)* 46, 578–588. doi:10.1111/j.1537-2995.2006.00776.x

Gravenor, M. B., McLean, A. R., and Kwiatkowski, D. (1995). The regulation of malaria parasitaemia: parameter estimates for a population model. *Parasitology* 110, 115–122. doi:10.1017/s0031182000063861

Greischar, M. A., Mideo, N., Read, A. F., and Bjørnstad, O. N. (2016). Predicting optimal transmission investment in malaria parasites. *Evolution* 70, 1542–1558. doi:10.1111/evo.12969

Gronowicz, G., Swift, H., and Steck, T. L. (1984). Maturation of the reticulocyte in vitro. *J. Cell Sci.* 71, 177–197. doi:10.1242/jcs.71.1.177

Haydon, D. T., Matthews, L., Timms, R., and Colegrave, N. (2003). Top-down or bottom-up regulation of intra–host blood–stage malaria: do malaria parasites most resemble the dynamics of prey or predator? *Proc. R. Soc. Lond. B* 270, 289–298. doi:10.1098/rspb.2002.2203

Hellriegel, B. (1992). Modelling the immune response to malaria with ecological concepts: short-term behaviour against long-term equilibrium. *Proc. R. Soc. Lond. B* 250, 249–256. doi:10.1098/rspb.1992.0156

Hetzel, C. and Anderson, R. M. (1996). The within-host cellular dynamics of bloodstage malaria: theoretical and experimental studies. *Parasitology* 113, 25–38. doi:10.1017/s0031182000066245

Ionides, E. L., Nguyen, D., Atchadé, Y., Stoev, S., and King, A. A. (2015). Inference for dynamic and latent variable models via iterated, perturbed Bayes maps. *Proc. Natl. Acad. Sci.* 112, 719–724. doi:10.1073/pnas.1410597112

Jakeman, G. N., Saul, A., Hogarth, W. L., and Collins, W. E. (1999). Anaemia of acute malaria infections in non-immune patients primarily results from destruction of uninfected erythrocytes. *Parasitology* 119, 127–133. doi:10.1017/s0031182099004564

Jarra, W. and Brown, K. N. (1989). Invasion of mature and immature erythrocytes of CBA/Ca mice by a cloned line of *Plasmodium chabaudi chabaudi*. *Parasitology* 99, 157–163. doi:10.1017/s0031182000058583

Kamiya, T., Davis, N. M., Greischar, M. A., Schneider, D., and Mideo, N. (2021). Linking functional and molecular mechanisms of host resilience to malaria infection. *Elife* 10, e65846. doi:10.7554/elife.65846

Khoury, D. S., Aogo, R., Randriafanomezantsoa-Radohery, G., McCaw, J. M., Simpson, J. A., McCarthy, J. S., et al. (2018). Within-host modeling of blood-stage malaria. *Immunol. Rev.* 285, 168–193. doi:10.1111/imr.12697

King, A. A., Nguyen, D., and Ionides, E. L. (2016). Statistical inference for partially observed Markov processes via the R package pomp. *J. Stat. Softw.* 69, 1–43. doi:10.18637/jss.v069.i12

Klei, T., Van Bruggen, R., Dalimot, J., Veldthuis, M., Mul, E., Rademakers, T., et al. (2019). Hemolysis in the spleen drives erythrocyte turnover. *Blood* 134, 946. doi:10.1182/blood-2019-124342

Kochin, B. F., Yates, A. J., de Roode, J. C., and Antia, R. (2010). On the control of acute rodent malaria infections by innate immunity. *PLoS ONE* 5, e10444. doi:10.1371/journal.pone.0010444

Lamb, T. J. and Langhorne, J. (2008). The severity of malarial anaemia in *Plasmodium chabaudi* infections of BALB/c mice is determined independently of the number of circulating parasites. *Malar. J.* 7, 1–9. doi:10.1186/1475-2875-7-68

Libregts, S. F., Gutiérrez, L., de Bruin, A. M., Wensveen, F. M., Papadopoulos, P., van Ijcken, W., et al. (2011). Chronic IFN-γ production in mice induces anemia by reducing erythrocyte life span and inhibiting erythropoiesis through an irf-1/pu.1 axis. *Blood* 118, 2578–2588. doi:10.1182/blood-2010-10-315218

Lim, C., Hansen, E., DeSimone, T. M., Moreno, Y., Junker, K., Bei, A., et al. (2013). Expansion of host cellular niche can drive adaptation of a zoonotic malaria parasite to humans. *Nat. Commun.* 4, 1638. doi:10.1038/ncomms2612

Lin, J.-w., Sodenkamp, J., Cunningham, D., Deroost, K., Tshitenge, T. C., McLaughlin, S., et al. (2017). Signatures of malaria-associated pathology revealed by high-resolution whole-blood transcriptomics in a rodent model of malaria. *Sci. Rep.* 7, 41722. doi:10.1038/srep41722

Mackinnon, M. J. and Read, A. F. (1999). Genetic relationships between parasite virulence and transmission in the rodent malaria *Plasmodium chabaudi*. *Evolution* 53, 689–703. doi:10.2307/2640710

McQueen, P. G. and McKenzie, F. E. (2004). Age-structured red blood cell susceptibility and the dynamics of malaria infections. *Proc. Natl. Acad. Sci.* 101, 9161–9166. doi:10.1073/pnas.0308256101

Metcalf, C. J. E., Graham, A. L., Huijben, S., Barclay, V. C., Long, G. H., Grenfell, B. T., et al. (2011). Partitioning regulatory mechanisms of within-host malaria dynamics using the effective propagation number. *Science* 333, 984–988. doi:10.1126/science.1204588

Metcalf, C. J. E., Long, G. H., Mideo, N., Forester, J. D., Bjørnstad, O. N., and Graham, A. L. (2012). Revealing mechanisms underlying variation in malaria virulence: effective propagation and host control of uninfected red blood cell supply. *J. R. Soc. Interface* 9, 2804–2813. doi:10.1098/rsif.2012.0340

Mideo, N., Barclay, V. C., Chan, B. H. K., Savill, N. J., Read, A. F., and Day, T. (2008). Understanding and predicting strain-specific patterns of pathogenesis in the rodent malaria *Plasmodium chabaudi*. *Am. Nat.* 172, E214–E238. doi:10.1086/591684

Miller, M. R., Råberg, L., Read, A. F., and Savill, N. J. (2010). Quantitative analysis of immune response and erythropoiesis during rodent malarial infection. *PLoS Comput. Biol.* 6, e1000946. doi:10.1371/journal.pcbi.1000946

Mosquera, J. and Adler, F. R. (1998). Evolution of virulence: a unified framework for coinfection and superinfection. *J. Theor. Biol.* 195, 293–313. doi:10.1006/jtbi.1998.0793

Mourão, L. C., Baptista, R. d. P., de Almeida, Z. B., Grynberg, P., Pucci, M. M., Castro-Gomes, T., et al. (2018). Anti-band 3 and anti-spectrin antibodies are increased in *Plasmodium vivax* infection and are associated with anemia. *Sci. Rep.* 8, 8762. doi:10.1038/s41598-018-27109-6

Ney, P. A. (2011). Normal and disordered reticulocyte maturation. *Curr. Opin. Hematol.* 18, 152. doi:10.1097/moh.0b013e328345213e

Nowak, M. A. and May, R. M. (1994). Superinfection and the evolution of parasite virulence. *Proc. R. Soc. Lond. B* 255, 81–89. doi:10.1098/rspb.1994.0012

Pak, D., Kamiya, T., and Greischar, M. A. (2023). Proliferation in malaria parasites: how resource limitation can prevent evolution of greater virulence. *bioRxiv* doi:10.1101/2023.12.16.571859

Paulson, R. F., Hariharan, S., and Little, J. A. (2020). Stress erythropoiesis: definitions and models for its study. *Exp. Hematol.* 89, 43–54. doi:10.1016/j.exphem.2020.07.011

Peters, M. A. E., Greischar, M. A., and Mideo, N. (2021). Challenges in forming inferences from limited data: a case study of malaria parasite maturation. *J. R. Soc. Interface* 18, 20210065. doi:10.1098/rsif.2021.0065

R Core Team (2022). *R: A Language and Environment for Statistical Computing*. R Foundation for Statistical Computing, Vienna, Austria

Ruan, B. and Paulson, R. F. (2023). Metabolic regulation of stress erythropoiesis, outstanding questions, and possible paradigms. *Front. Physiol.* 13, 1063294. doi:10.3389/fphys.2022.1063294

Thakre, N., Fernandes, P., Mueller, A.-K., and Graw, F. (2018). Examining the reticulocyte preference of two Plasmodium berghei strains during blood-stage malaria infection. *Front. Microbiol.* 9, 166. doi:10.3389/fmicb.2018.00166

Timms, R., Colegrave, N., Chan, B. H. K., and Read, A. F. (2001). The effect of parasite dose on disease severity in the rodent malaria *Plasmodium chabaudi*. *Parasitology* 123, 1–11. doi:10.1017/s0031182001008083

van Baalen, M. and Sabelis, M. W. (1995). The dynamics of multiple infection and the evolution of virulence. *Am. Nat.* 146, 881–910. doi:10.1086/285830

Wale, N., Jones, M. J., Sim, D. G., Read, A. F., and King, A. A. (2019). The contribution of host cell-directed vs. parasite-directed immunity to the disease and dynamics of malaria infections. *Proc. Natl. Acad. Sci.* 2018, 201908147. doi:10.1073/pnas.1908147116

Wale, N., Sim, D. G., and Read, A. F. (2017). A nutrient mediates intraspecific competition between rodent malaria parasites in vivo. *Proc. R. Soc. Lond. B* 284, 20171067. doi:10.1098/rspb.2017.1067

Wiczling, P. and Krzyzanski, W. (2008). Flow cytometric assessment of homeostatic aging of reticulocytes in rats. *Exp. Hematol.* 36, 119–127. doi:10.1016/j.exphem.2007.09.002

Wood, S. N. (2017). *Generalized Additive Models: An Introduction with R* (Chapman and Hall/CRC), 2 edn. doi:10.1201/9781315370279

Yap, G. S. and Stevenson, M. M. (1992). *Plasmodium chabaudi* AS: erythropoietic responses during infection in resistant and susceptible mice. *Exp. Parasitol.* 75, 340–352. doi:10.1016/0014-4894(92)90219-z

Yap, G. S. and Stevenson, M. M. (1994). Blood transfusion alters the course and outcome of *Plasmodium chabaudi* AS infection in mice. *Infect. Immun.* 62, 3761–3765. doi:10.1128/iai.62.9.3761-3765.1994

Table 1. Functional forms commonly used to describe red blood cell (RBC) supply and uninfected RBC clearance during malaria infections. Numbering corresponds to example functional forms displayed in Figure 1. *Neither RBC supply nor RBC destruction are explicitly described. **Clearance occurs through aging out of the oldest RBC class.

	Reference	RBC supply	RBC clearance
1	Anderson et al. (1989)	Constant	Increasing linear function of erythrocyte density
2	Antia et al. (2008)	Hill function, based on 2.5 day lagged erythrocyte density	Constant**
3	Gravenor et al. (1995)	Constant	Increasing linear function of erythrocyte density
4	Greischar et al. (2016)	Increasing linear function of current erythrocyte deficit (i.e., decreasing function of current erythrocyte density)	Increasing linear function of erythrocyte density
5	Haydon et al. (2003)	Increasing linear function of current erythrocyte deficit	Unspecified
6	Hellriegel (1992)	Constant	Increasing linear function of erythrocyte density
7	Hetzel and Anderson (1996)	Constant	Increasing linear function of erythrocyte density
8	Jakeman et al. (1999)	Time-varying; constant; no supply	Time-varying; senescence only
9	Kamiya et al. (2021)	Constant with additional supply increasing with 2 day lagged erythrocyte deficit	Constant baseline mortality, additional clearance scaling with parasite density
10	Khoury et al. (2018)	Constant or decreasing linear function of current erythrocyte density	Increasing linear function of erythrocyte density
11	Lim et al. (2013)	Constant	Increasing linear function of erythrocyte density
12	McQueen and McKenzie (2004)	Time-varying	Constant**
13	Metcalf et al. (2011)	Linear*	Linear*
14	Metcalf et al. (2012)	Time-varying*	Time-varying*
15	Mideo et al. (2008)	Increasing linear function of 1-4 day lagged erythrocyte deficit	Constant fraction
16	Miller et al. (2010)	Decreasing linear function of erythrocyte density plus upregulation based on 0-6 day lagged erythrocyte deficit	Increasing linear function of erythrocyte density
17	Thakre et al. (2018)	Time-varying	Time-varying
18	Wale et al. (2019)	Time-varying	Time-varying

TABLES

Table 2. Model forms considered for the relationship between R_t and E_{t-1}. We fit each of the following six models using 5 different breakpoints (i.e., days 8, 9, 10, 11; no breakpoint), for a total of 30 different models. Note that when no breakpoint is specified, the phase term becomes irrelevant so that, for example, model F becomes equivalent to the uniphasic, linear model commonly used in previously published predictive models (cf. Figure 1). Note that pABA is treated as a discrete factor. Note that to address the issue of multicollinearity associated with regressing against higher order polynomials, we opted to use orthogonal polynomials for model fitting.

Model	Form	
A	$R_t \sim E_{t-1}^2 : \text{pABA} : \text{phase} + E_{t-1} : \text{pABA} : \text{phase} + \text{pABA} : \text{phase}$	
B	$R_t \sim E_{t-1}^2 : \text{phase} + E_{t-1} : \text{phase} + \text{pABA} : \text{phase}$	
C	$R_t \sim E_{t-1}^2 : \text{phase} + E_{t-1} : \text{phase} + \text{phase}$	
D	$R_t \sim E_{t-1} : \text{pABA} : \text{phase} + \text{pABA} : \text{phase}$	$\times 5$ breakpoints
E	$R_t \sim E_{t-1} : \text{phase} + \text{pABA} : \text{phase} + \text{phase}$	
F	$R_t \sim E_{t-1} : \text{phase} + \text{phase}$	

Table 3. Model forms considered for predicting clearance rate Q^{un} as a function of time and a parasite nutrient pABA. Model fitting was performed using the `gam` function from the **mcgv** package (Wood, 2017) in **R** (R Core Team, 2022), which fits a generalized additive model to data.

Model	Form
A	$Q^{\text{un}} \sim \text{gam}(\text{s}(\text{time}, \text{by} = \text{pABA}) + \text{pABA})$
B	$Q^{\text{un}} \sim \text{gam}(\text{s}(\text{time}))$
C	$Q^{\text{un}} \sim 1$
D	$Q^{\text{un}} \sim \text{gam}(E_t)$
E	$Q^{\text{un}} \sim \text{gam}(E_t : \text{pABA} + \text{pABA})$

FIGURES

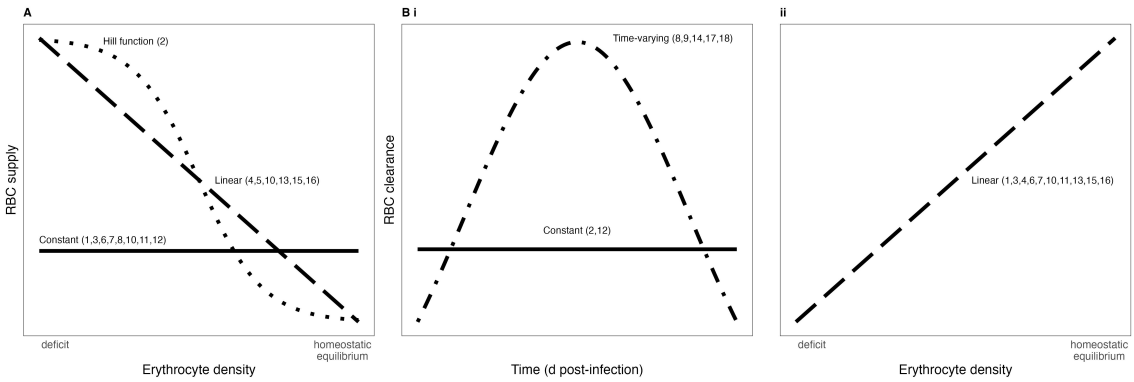

Figure 1. Functional forms commonly used to describe RBC supply and uninfected RBC clearance during malaria infections. Numbers associated with each functional form correspond to references in Table 1.

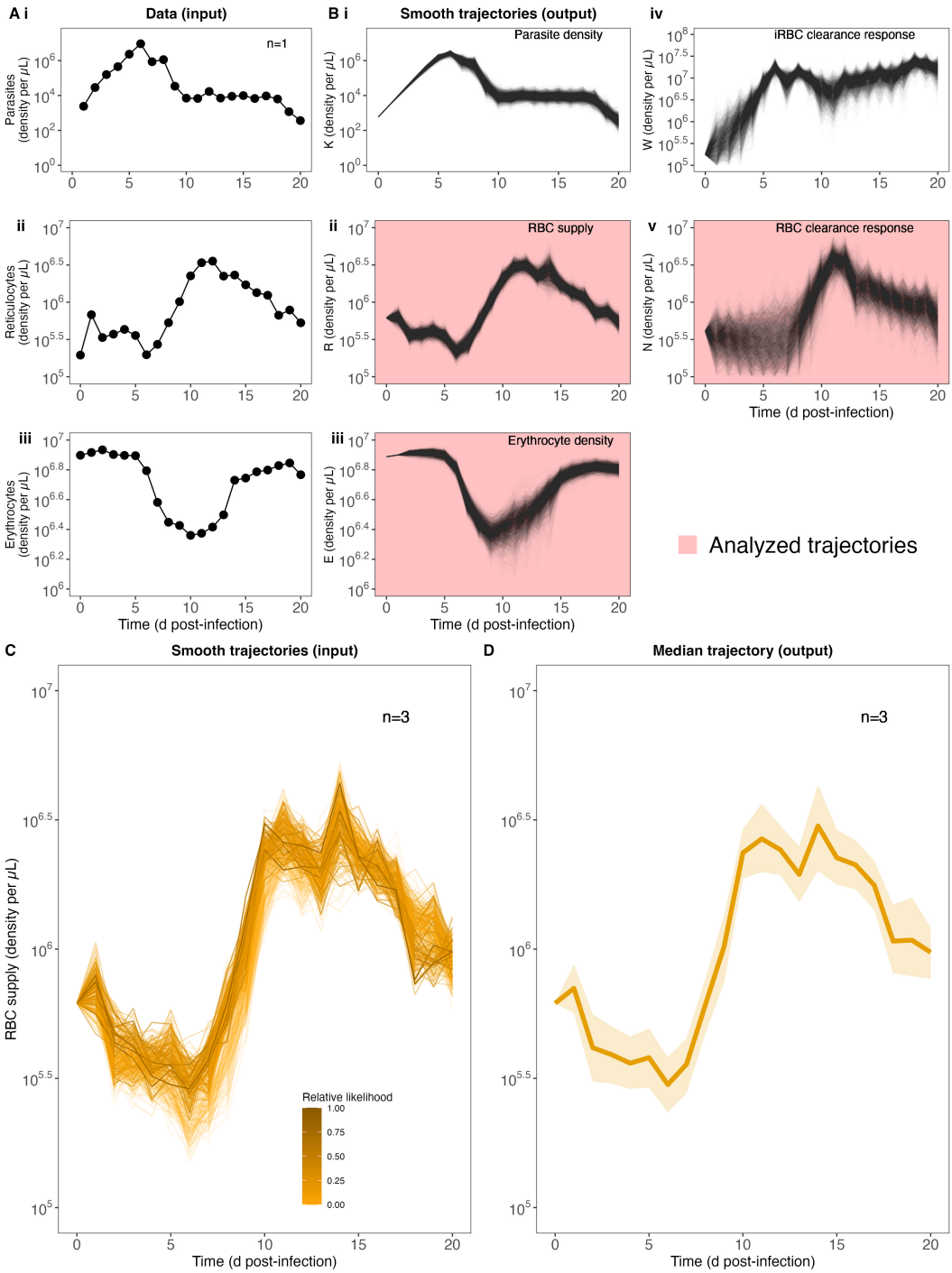

Figure 2. Quantifying RBC supply and clearance using a data-transformation scheme. A) Raw data of parasite density, reticulocyte supply and erythrocyte density from day 0 to day 20 post-infection for 1 mouse, infected with *Plasmodium chabaudi*. B) Model fits (2000 in total) produced by fitting the data-transformation scheme to the raw data for the single mouse shown in (A). Note for our analyses we consider the model fits of variables R, E and N, whose panels are shaded. C) Reticulocyte supply according to the model fits (300 of 2000 shown for visibility) produced by fitting the data-transformation scheme to the raw data for each of the three mice from the unsupplemented (0%) pABA treatment. The color and opacity of each model fit represents its relative likelihood. D) Treatment-level model fit for reticulocyte supply given the individual model fits for the unsupplemented pABA treatment displayed in (C). The series represents the median model fit, and shading gives the 90% confidence intervals.

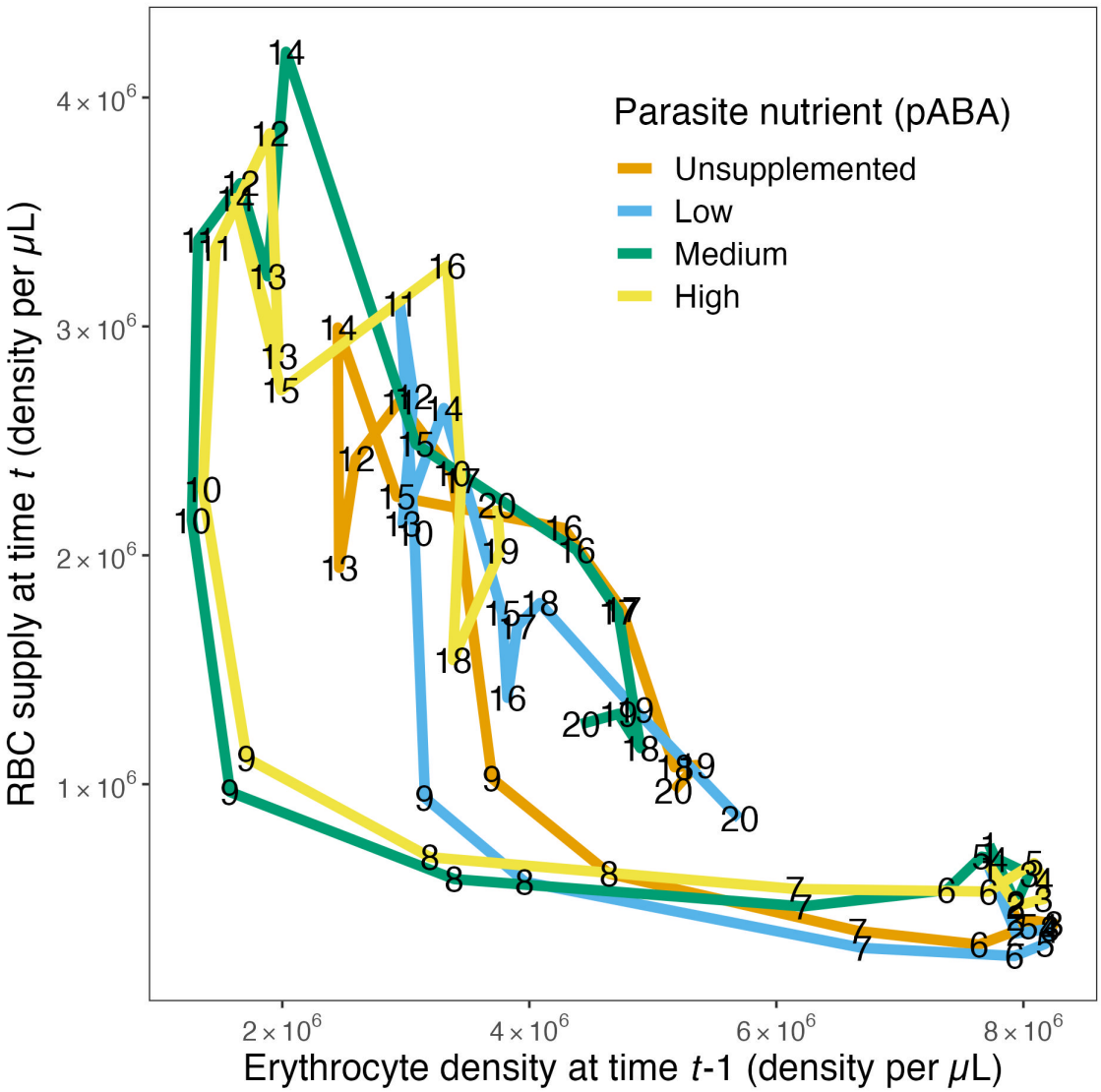

Figure 3. The RBC supply function does not take the form of a single function, as is commonly assumed. The relationship between erythrocyte density on day $t-1$ and RBC supply (reticulocyte density) on day t for each of the four parasite nutrient (pABA) treatments. The paths are labelled with time t, i.e., a point on the path labelled 8 shows the RBC supply on day 8, given the erythrocyte supply on day 7.

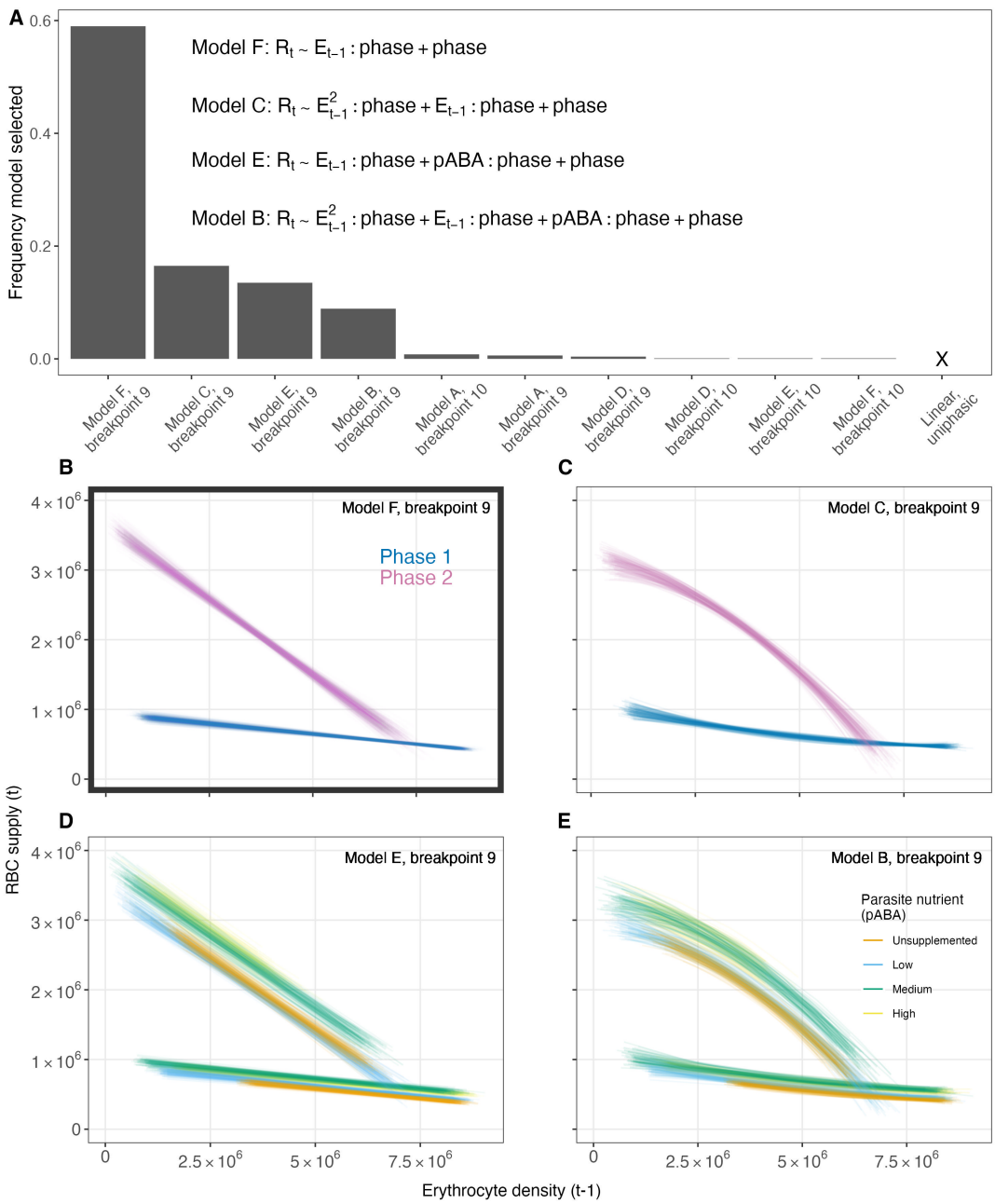

Figure 4. RBC supply during *P. chabaudi* infection occurs in two distinct phases and may change with parasite growth rate. A) Frequency of 10 models selected via AIC. Equations for the top four selected models are included (as well as featured in Table 2). Note i) the top four models agree on a breakpoint at day 9 post-infection and ii) only 10 of the 30 total models were selected at non-zero frequency. Importantly, a uniphasic, linear model was never selected. B-D) Predicted values according to the top four models. The range of predicted values for different treatments differ, as we obtained model predictions based on the ranges of observed erythrocyte densities for each treatment. Colors for predicted values in B-C) reflect two distinct phases in RBC supply (with a breakpoint at day 9), while colors for predicted values in D-E) reflect parasite nutrient (pABA) treatments.

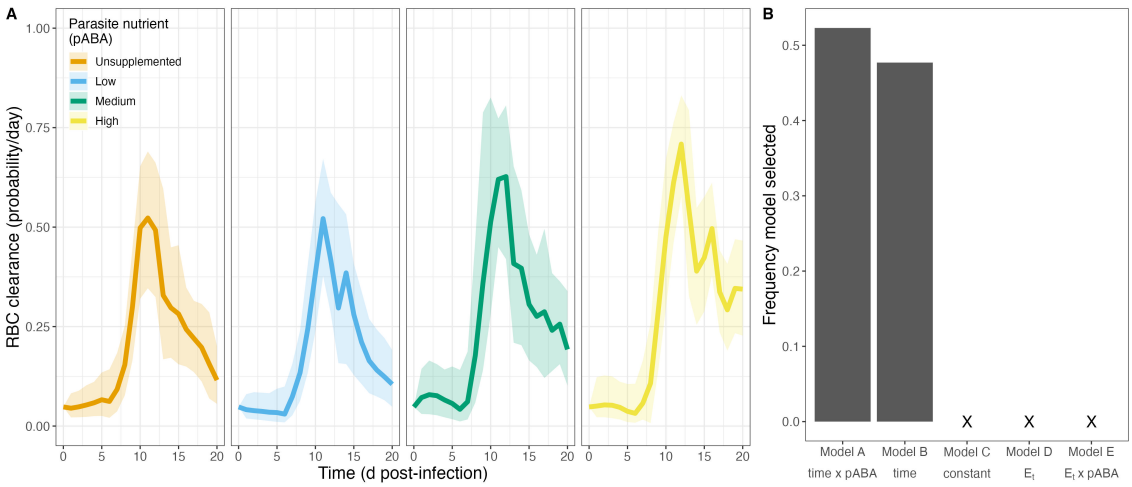

Figure 5. Clearance rates of uninfected RBCs during *P. chabaudi* infection vary through time and with a parasite nutrient (and thus growth rate). A) Median treatment-level red blood cell (RBC) clearance rates over time, in each of four groups of mice that received a different concentration of the parasite nutrient pABA. B) Frequency of 5 models selected via AIC. Note that a model including a linear relationship between clearance rate and E_t was never selected.